Chemical composition and vasodilator activity of different Alpinia zerumbet leave extracts, a potential source of bioactive flavonoids.

Munyck A. da Silva[1] · Lenize C. R. M. de Carvalho[2] · Cristiane P. Victório[3] · Dayane T. Ognibene[2] · Angela C. Resende[2] · Marcelo A. V. de Souza[4]

✉ Munyck A. da Silva

munyckdsc@gmail.com

[1] Department of Organic Chemistry, Chemistry Institute, State University of Rio de Janeiro, 20550-900, Rio de Janeiro-RJ, Brazil.

[2] Department of Pharmacology, Biology Institute, State University of Rio de Janeiro, 20550-900, Rio de Janeiro-RJ, Brazil.

[3] University Unit of Biology, West Zone State University, 23070-200, Rio de Janeiro-RJ, Brazil.

[4] Department of Chemical Process, Chemistry Institute, State University of Rio de Janeiro, 20550-900, Rio de Janeiro-RJ, Brazil.

Abstract

A polyphenol-rich extract with an expressive vasodilator effect was obtained from fresh leaves of *Alpinia zerumbet* (AZ), a medicinal plant. The vasodilator effects of AZ obtained from different extraction conditions were studied in perfused mesenteric vascular bed, and total polyphenol content (TPC) was determined for all samples. Chemical composition of AZ was analyzed by UHPLC/ESI-QTOF-MS, and a list of putative compounds was obtained by a molecular network. Briefly, results obtained indicate a 50% hydroethanolic extract from fresh leaves (AZE4) as the best extraction condition, presenting the greatest vasodilator effect (ED 50 = 7.1 µg ± 1.73) and TPC (16.30 mg GAE/g ± 0.44). Flavonoids were detected as main constituents and alpinetin, kaempferol-3-O-glucuronide, (-)- epicatechin and pinocembrin were identified as major compounds. The last effective extraction condition was 50% hydroethanolic extract from dried leaves without heating, which showed the smallest vasodilator response (ED 50 = 29.1 µg ± 4.3) and TPC (6.35 mg GAE/g ± 0.08), reinforcing the use of fresh leaves and heating step to improve extracts performance. The vasodilator effect and the main flavonoid composition of AZE4 provide experimental support for the indication of this extract as a potential source of bioactive flavonoids for the treatment of cardiovascular diseases.

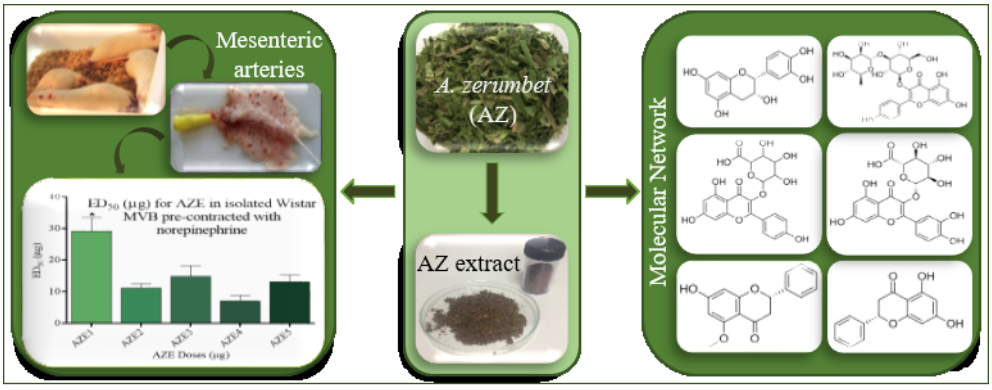

Keywords: *Alpinia zerumbet* · hypertension · mesenteric vascular bed · flavonoids · Q-TOF.

Abbreviations

ACh	Acetylcholine
AZ	*Alpinia zerumbet*
AZE	*Alpinia zerumbet* extracts
cGMP	Cyclic guanosine monophosphate
GA	Gallic acid
GNPS	Global Natural Products Social Molecular Networking
I3ON	Isorharmnetin-3-O-neohesperidoside
K3OG	Kaempferol-3-O-glucuronide
K3OG3R	Kaempferol-3-O-glucoside-3"-rhamnoside
LDL	Low-density lipoprotein
MN	Molecular networking
MVB	Mesenteric vascular bed
NE	Norepinephrine
NF-κB	Nuclear factor kappa-light-chain-enhancer of activated B cells
NG	Nitroglycerine
PSS	Physiological salt solution
Q3OG	Quercetin-3-O-glucuronide
RDA	Retro-Diels Alder
ROS	Reactive oxygen species
SEM	Standard error of the mean
TIC	Total ion chromatogram
TPC	Total polyphenol content

Introduction

The medicinal plant *Alpinia zerumbet* (AZ) is originated from West Asia, and is widespread in the northeast and southeast of Brazil. Leaves of AZ are widely used as a popular treatment for hypertension [1], and approximately 80 % of the population of developing countries use herbal medicines treatments as a first option [2]. Hypertension is considered a global public health problem, affecting more than 1 billion people, with a potential risk of heart attacks [2]. In the context of folk medicine, the use of AZ is recognized for its diuretic and antihypertensive properties, besides anti-inflammatory action [3,4], which may contribute to reducing risks of cardiovascular diseases.

Extensive research has shown essential oil extracts of AZ [4,5] may act as a preventive treatment for skin diseases [6], present inhibitor properties on low-density lipoprotein (LDL) [7], vasodilator, and antihypertensive effects [8], and protects endothelial cells minimizing the oxidative stress caused by LDL [4]. However, the vasodilator activity of hydroethanolic and aqueous extracts leaves is not widely reported.

The literature on the cardiovascular properties of *Alpinia zerumbet* reports a vasorelaxant effect of the essential oil of this plant [9] or its methanolic fraction [8], which does not represent the popular use of leaves infusion for hypertension treatment. On the other hand, our study focused on evaluating the procedures used in folk medicine to prepare extracts of *Alpinia zerumbet* leaves.

In this study, we evaluated the vasodilator effect of the 50% hydroethanolic and aqueous extracts obtained from AZ in the isolated mesenteric vascular bed (MVB) from male Wistar rats, comparing dried and fresh leaves under heating or not and their total polyphenol content (TPC). Moreover, based on the large health benefits of flavonoids due to their anti-inflammatory, anti-mutagenic, antioxidative, and vasodilatory effects [10], the chemical composition of the extracts of AZ was analyzed.

Results and Discussion

The main goal of the present study was to investigate a significant vasodilatory effect of different extracts from leaves of *Alpinia zerumbet* on perfused MVB pre-contracted with norepinephrine, in order to confirm an important pharmacological property of this plant, traditionally used for cardiovascular disease treatment in folk medicine. To achieve this objective, AZ extracts were submitted to analytical steps, including determination of total polyphenol content (TPC) and UHPLC/ESI-QTOF-MS analyses. The relevance of AZE in this scenario is clearly supported by the current findings presented in this study, after evaluation and comparison of all results obtained from mesenteric vascular bed reactivity and annotated compounds obtained by analytical techniques. The rapid identification of major compounds present in all AZE was successfully achieved by dereplication in GNPS (Global Natural Products Social Molecular Networking) platform, and the distribution of these molecules per extract was clearly visualized by the use of Cytoscape, which allowed defining the best extraction condition as the one used in AZE4.

Leaves processing and extraction

The leaves drying process was satisfactory within ten days at room temperature, confirmed by the weight stabilization after this period. Each type of extract was performed in quadruplicate, to ensure sufficient material for all experiments, and the average yield was 6 % w/w/ extract.

Mesenteric vascular bed reactivity

Isolated rat MVB perfused with PSS (physiological salt solution) at 4 mL/min presented basal average perfusion pressure in a range of 25 to 30 mmHg. *In bolus* injection of 120 μmol of

KCl increased the perfusion pressure up to 80 mmHg, confirming the viability of MVB preparation. The addition of 30 μmol of NE (norepinephrine) in the PSS induced an increase of perfusion pressure, remaining constant in a range of 90 to 120 mmHg. Acetylcholine (Ach, 10 pmol) and nitroglycerine (NG, 10 nmol) induced a decrease in the perfusion pressure, confirming the integrity of endothelium and vascular smooth muscle, respectively. These results enabled the evaluation of vasodilator responses of AZE, and Fig. 1 shows the dose-response curves for each extract.

The comparison of these curves (Fig. 1) obtained after administration of increasing doses for each extract (0.1, 0.3, 1, 10, 30, 100, and 300 μg) shows that the maximal vasodilator response (approximately 80%) was obtained between 100-300 μg of AZE for all samples. Based on the ED_{50} absolute values of the extracts, it is possible to classify them in descending order of potency: AZE4, AZE2, AZE5, AZE3, and AZE1, although only AZE1 was significantly different from the others. Table 1 presents ED_{50} values expressed as mean ± SEM, n = 6. AZE1* significantly different from all other AZE ($P<0.05$; ANOVA).

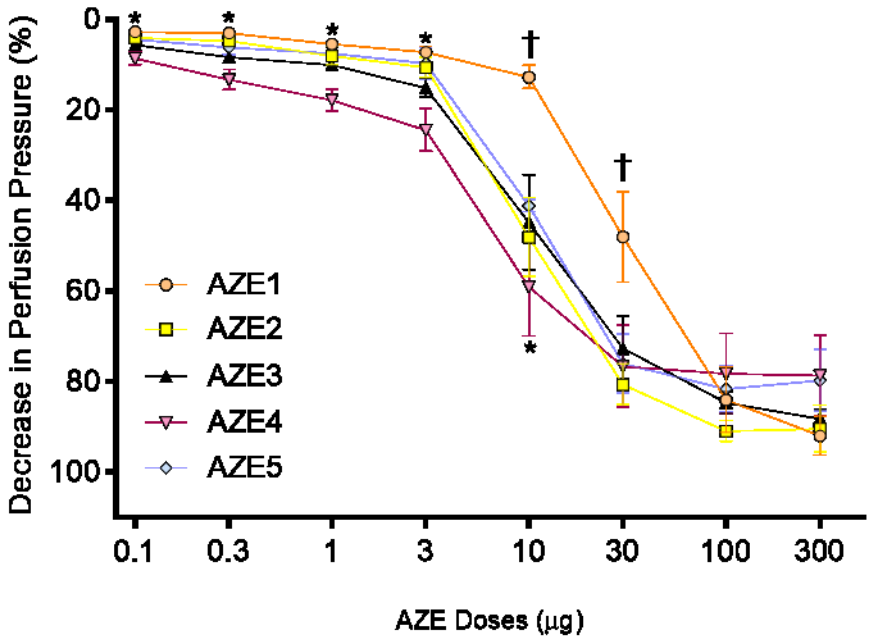

Fig. 1 Dose-dependent vasodilator effect induced by AZE in isolated MVB. Data are expressed as mean ± SEM, n = 6/ group. Using One-Way ANOVA and *post-hoc* test of Tukey: AZE4* significantly different ($P \leq 0.05$) when compared to AZE1, AZE2, AZE3, and AZE5. E2† significantly different ($P \leq 0.05$) when compared to AZE1

AZE1 presented the higher ED_{50} value ($P \leq 0.05$) compared to the other extracts, indicating the lowest potency among all extracts. AZE4 presented the lowest value for ED_{50} (7.1 µg±1.7), although not statistically different from the others. AZE4 vasodilator effect was significantly higher ($P \leq 0.05$) than the other extracts for doses < 30µg, indicating this extract as a more effective vasodilator than others. No significant differences were observed between the vasodilator responses of AZE2, AZE3, and AZE5.

Since AZE1 was the only extract prepared without heating, we suggest the lowest potency of the vasodilator effect of AZE1 could be in part attributed to the lack of heating in the procedure for the extract preparation. The solvents (water or hydroethanolic solution) used to prepare the different extracts and the type of leaves (fresh or dried), seem not to interfere

with the potency of the AZE2, AZE3, AZE4, and AZE5 extracts, since no statistical difference was observed between them. When the vasodilator effect is analyzed, it is possible to assume that the extracts obtained with fresh leaves (AZE3 and AZE4) are superior to those obtained with dried leaves (AZE1, AZE2, and AZE5). It is worth mentioning the AZE4 as the most effective vasodilator extract since it induced the greater vasodilator responses with doses below 30 μg when compared with the other extracts. The only evidence of a vasodilator effect in the same vascular preparation was previously described for a hydroethanolic extract obtained from dried leaves of *Alpinia zerumbet* without heating [11]. However, in the present study, the comparative evaluation suggested the extract AZE1 prepared exactly as this previous study was less effective as a vasodilator. Therefore, these findings show heating and the usage of fresh leaves in the extract preparation process are crucial to obtain an effective biological response.

Determination of total polyphenols by the Folin-Ciocaulteau method

Table 2 shows the total polyphenolic content for all AZE and AZE4 presented the highest total polyphenol content, followed by AZE3, AZE2, AZE5, and AZE1, in descending order. It is possible to assume that fresh leaves extracts retain more polyphenols (AZE4, AZE3), and the extraction solvent (water or hydroethanolic solution) does not affect this result. Results were expressed as mg of GA equivalent (GAE)/g of AZE, mean ± SEM, n = 3 for each sample.

Several experimental data have proposed polyphenols occurring naturally in many vegetables may participate in the mechanism of the biological effects of some medicinal plants [12]. Studies indicate natural polyphenols exert important actions on the cardiovascular system and maybe a potential source of new compounds to treat cardiovascular diseases [13]. Besides, the vasodilator effect of polyphenols has been extensively reported [14].

In the current study, the TPC of all AZE was determined to provide a possible correlation between their biological effects and the content of bioactive substances. Our results demonstrated AZE4 has the highest TPC, which correlates with their more effective vascular responses obtained in the perfused MVB. These findings corroborate our conclusion that both fresh leaves and heating are important variables for better extraction of the polyphenols leading to a more expressive vasodilator response. When all the extraction variables are evaluated, we can suggest hydroethanolic (AZE4) compared with the aqueous extract (AZE3) of the fresh leaves submitted to heating presented more expressive total polyphenol content and vasodilator response. Besides, it is important to mention that AZE1 showed the lowest TPC, which correlates with the smaller vasodilator response induced by the extract, and these values replicate the previously reported result [11].

AZE analysis and spectral library search at GNPS platform

The high-resolution mass spectral data provided an accurate measurement of exact mass for each molecule present on extracts, enabling a list of annotated compounds by library search at GNPS. Combining the libraries results obtained from GNPS and the correlation of mass fragments pathway described in literature data for each annotated molecule, the chemical profile of all AZE in the used extraction conditions could be investigated and compared.

GNPS spectral libraries were able to identify nine compounds, as listed in Table 3: D-(+)-Trehalose, (Epi)catechin, Procyanidin B2, Quercetin-3-O-glucuronide (Q3OG), Kaempferol-3-O-glucoside-3"-rhamnoside (K3OG3R), Kaempferol-3-O-glucuronide (K3OG), Isorharmnetin-3-O-neohesperidoside (I3ON), Alpinetin and Pinocembrin. Fig. 2 displays AZE total ion chromatograms (TIC) obtained from the tandem mass spectrometry system, where compounds are numbered according to Table 3. Peaks from methanol, used as solvent, and from the sodium formate, used as calibrant, are identified as B and C,

respectively. The Cytoscape view for all molecular network (MN) obtained and nodes representing annotated compounds distribution per extract is showed in Fig. 3.

The MN obtained from the analysis of all extracts indicates similar composition for AZE3, AZE4, and AZE5, while AZE1 presented only alpinetin, kaempferol-3-O-glucuronide, and kaempferol-3-O-glucoside-3"-rhamnoside, with the lowest intensities. This is in agreement with TPC and EC_{50} values previously described. In contrast, AZE4 and AZE5 presented all compounds annotated by GNPS, but AZE4 presented compounds in a higher percentage.

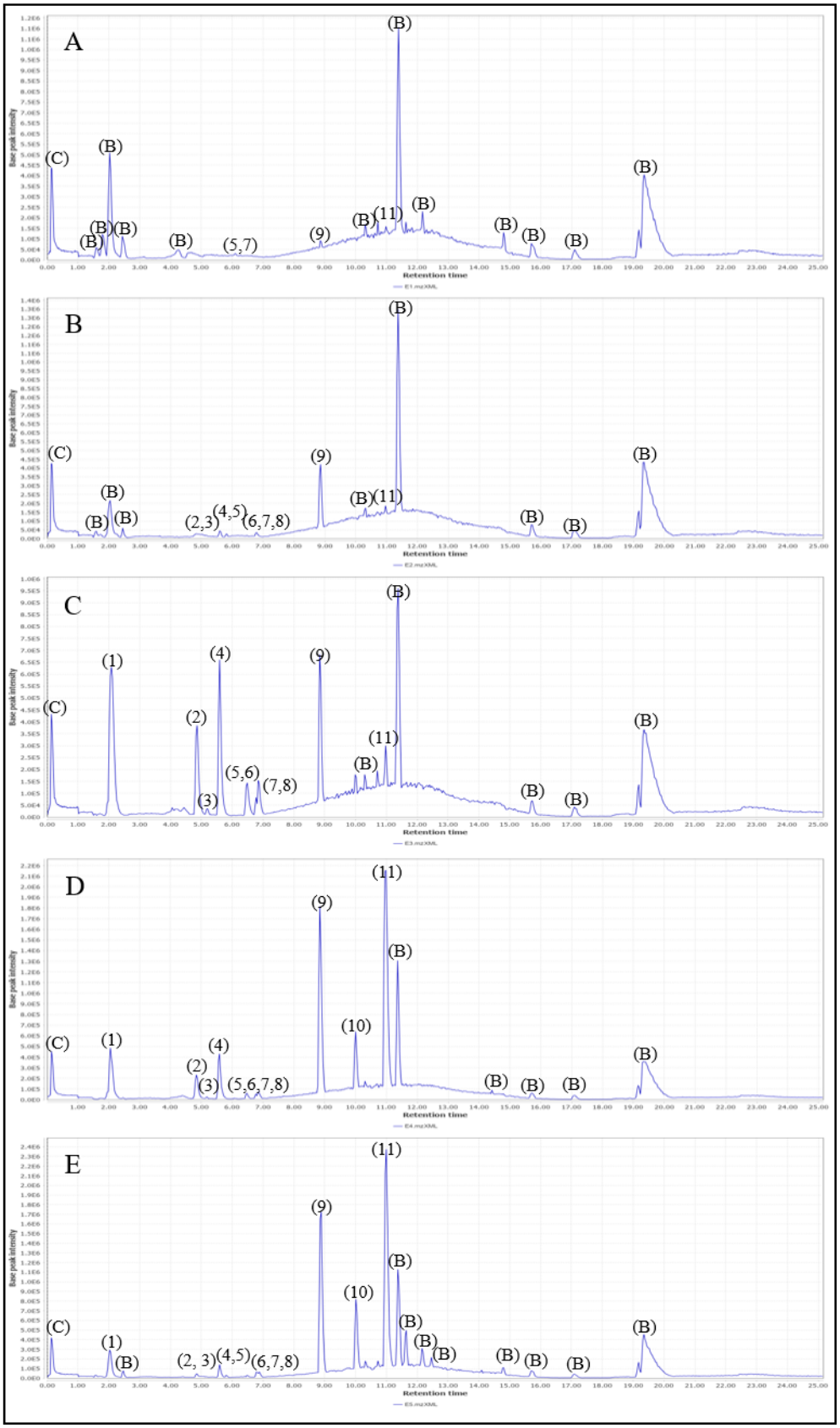

Fig. 2 The UHPLC/ESI-QTOF-MS (TIC) of *Alpinia zerumbet*: a) dried leaves hydroethanolic extract without heating (AZE1); b) dried leaves aqueous extract (AZE2); c) fresh leaves

aqueous extract (AZE3); d) fresh leaves hydroethanolic extract (AZE4) and e) dried leaves hydroethanolic extract (AZE5). Compounds peaks annotated by GNPS are as follow: D-(+)-Trehalose (1), (Epi)catechin (isomer) (2), Procyanidin B2 (3), (Epi)catechin (isomer) (4), Quercetin-3-O-glucuronide (5), Kaempferol-3-O-glucoside-3"-rhamnoside (6), Kaempferol-3-O-glucuronide (7), Isorharmnetin-3-O-neohesperidoside (8), Alpinetin isomer (9), Pinocembrin (10), Alpinetin isomer (11). Sodium formate was used as calibrant (C) and methanol as blank (B)

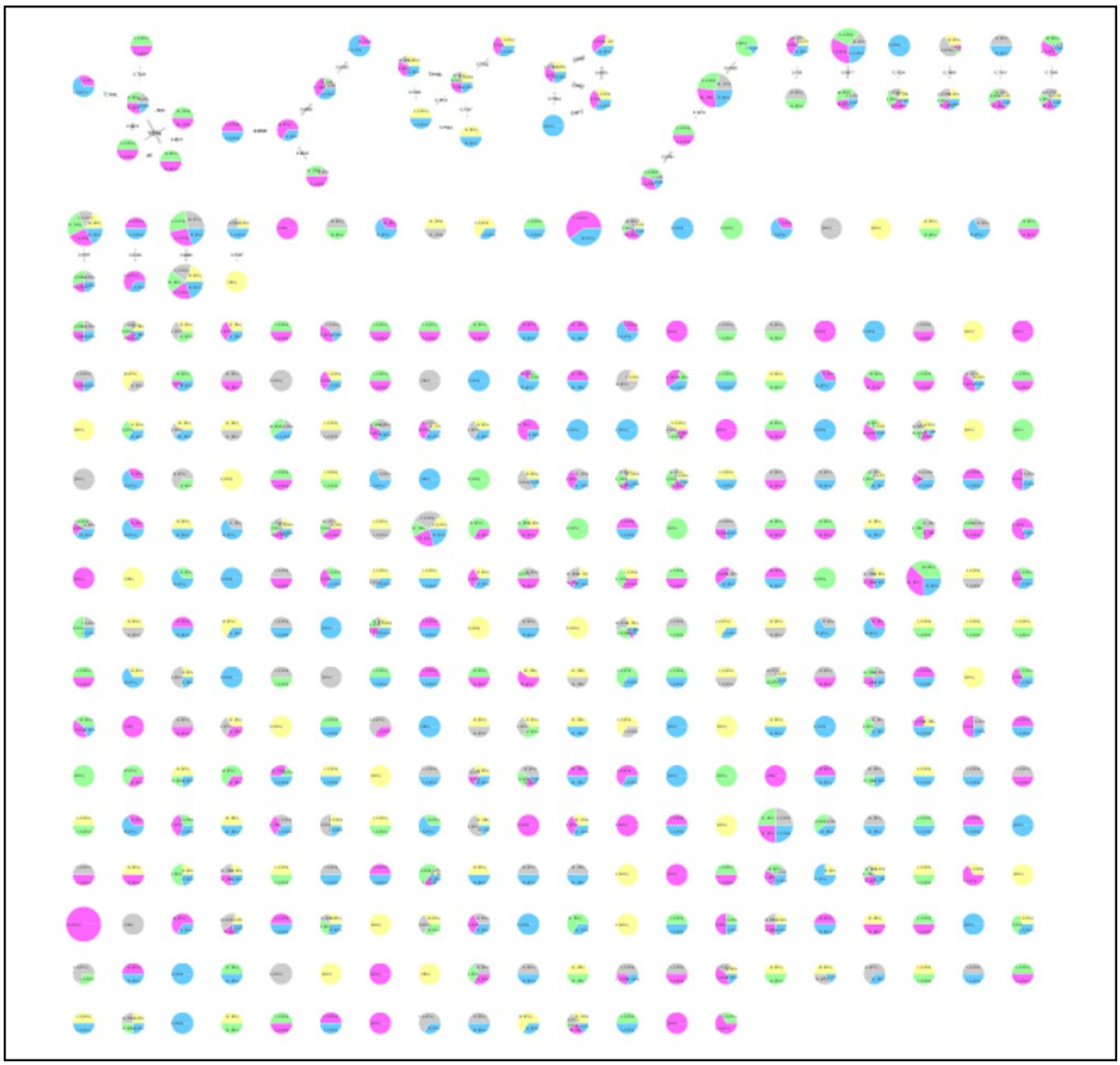

Fig. 3 Cytoscape view of entire molecular network and nodes of major compounds annotated by GNPS

Compound 1 was annotated by GNPS as D-(+)-Trehalose (Fig. 4), a non-reducing sugar that may present several isomers. However, as described by Verardo [15] it is possible to distinguish these compounds by formate adducts $[M+HCOO]^-$ fragmentation pathway at m/z 387. Besides that, non-reducing sugars like D-(+)-Trehalose present characteristics fragments at m/z 341$[M-H]^-$ ion of sucrose [16], m/z 179, formed through glycoside bond cleavage [16], also exhibiting ions (MS^3; 387 → 341 →) at m/z 179 (base peak), 161, 113, 101 [15]. All of these fragments could be observed in the mirror match tool from GNPS, with score of 73% in terms of correlation of cosine with reference spectrum.

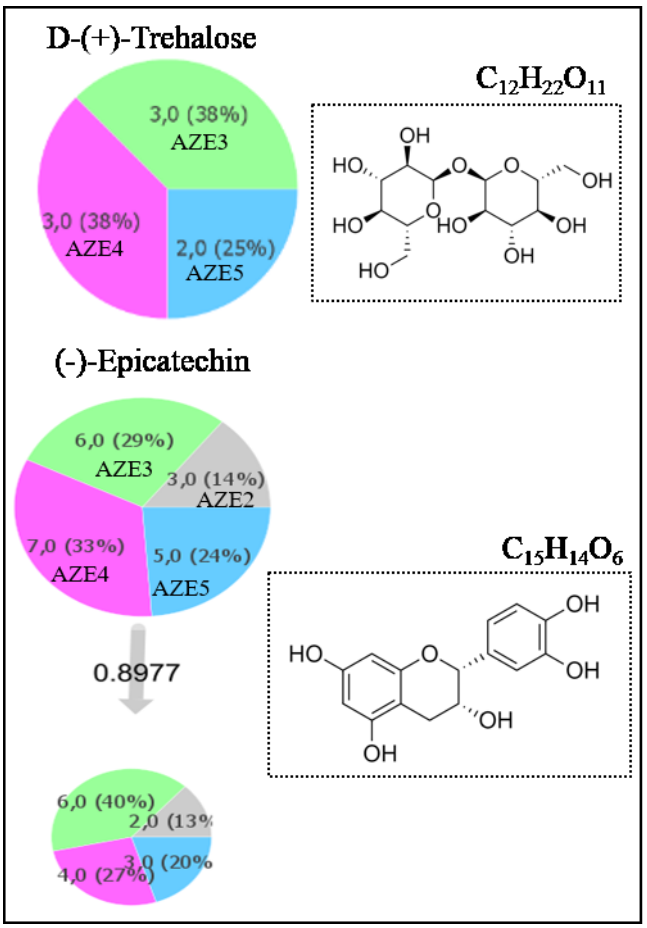

Fig. 4 Cytoscape view of D-(+)-Trehalose and (-)Epicatechin nodes annotated by GNPS. Cytoscape converted the abundance data obtained from each AZE TIC to percentages. AZE3 and AZE 4 contribute with 38% and AZE5 contributes with 25% of all D-(+)-Trehalose found in the molecular network. AZE4 contributes with 33%, AZE3 with 29%, AZE5 with 24% and AZE2 with 14% of all (-)-Epicatechin found in the molecular network

Catechins are classified as flavonols [17] presenting two chiral centers on the molecule, i.e., four possible diastereoisomers: two stereoisomers with trans configuration ((±)-catechin), and two stereoisomers presenting cis configuration ((±)-epicatechin). Tsao [17] mentions (+)-catechin and (−)-epicatechin as the two isomers often found in food plants, which could explain GNPS annotation for Compound 2 as (-)epicatechin (Fig. 4). Hence, the most effective strategy for identifying each of these peaks in 4.84 and 5.59 minutes as (+)-catechin or (−)-epicatechin would be through comparison with analytical standards analysis of these isomers, since they present the same fragmentation profile in the mass spectra. By means of this, this annotated compound by GNPS will be referred as (epi)catechin isomer in the current paper. Both compounds at the mentioned retention times present m/z 289 as base peak [18]. The MS^2 spectrum of this fragment, presented ions at m/z 245 $[M - H - 44]^-$, that could be attributed to the loss of $–CH_2–CHOH–$ or CO_2 moieties, and at m/z 205 and 179 due to the loss of the flavonoid A ring [M − H − 84]− and B ring $[M - H - 110]^-$, respectively. [18]. All of these characteristic catechin markers could be observed in the mirror match tool from GNPS, with score of 90% in terms of correlation of cosine with reference spectrum for (-)epicatechin molecule.

A recent study [19] reported the synergic effect of (epi)catechin isomer and D-(+)-Trehalose as inhibitors of platelet activity and oxidative stress. This may be achieved through increasing NO bioavailability and reducing risk factors of cardiovascular diseases when used

as a treatment in patients with metabolic syndrome. These two compounds were annotated in AZE3, AZE4, AZE5, and AZE4 presented the highest contribution in MN for (epi)catechin isomer (33%). Several studies describe the cardioprotective effects of epicatechin by reducing systemic blood pressure, platelet activation, and thrombus formation increase of endothelial-driven vasodilatory response in a dose-dependent manner [20–22]. A mechanism for this action was proposed, considering that epicatechin relaxed isolated human arteries via hyperpolarization through different K^+ channels, as well as by interference with Ca^{2+} [23] . Furthermore, (epi)catechin isomer and its dimer procyanidin B2 (Fig. 5), annotated for AZE4 in the highest percentage in MN, also contribute in a synergic mode to promote beneficial effects on the heart cardiovascular system by directly influencing mitochondrial functions. Besides that, procyanidin B2 presents anti-inflammatory and antioxidant properties [24], as well as a potent endothelium-dependent vasodilator effect on the isolated human blood vessels, because of an increase in NO synthesis [23]. These findings were also observed in isolated human saphenous veins [25].

Procyanidin B2 (Compound 3 at 5.18 minutes, Fig. 5) presents m/z 577 $[M-H]^-$, as base peak in MS^1 spectra, characteristic of dimeric proanthocyanidins [26]. Analyzing the MS^2 spectrum of this fragment, it is possible to confirm major product ions at 451, 425, 407 and 289 m/z [26]. A loss of 126 mass unit corresponding to the heterocyclic ring fission (HRF) fragmentation formed m/z 451 [26]. The ion at m/z 425 $[M-152-H]^-$ was due to retro-Diels-Alder fragmentation (RDA). According to Maldini [26], this RDA yielded the product ion at m/z 407 $[M-152-18-H]^-$ due to the neutral loss of the water. Finally, the ion at m/z 289 was attributed to Quinone methide (QM) fragmentation [M-288-H] [26]. In this case, the spectral similarity was obtained with score of 86% in terms of cosine correlation with reference spectrum.

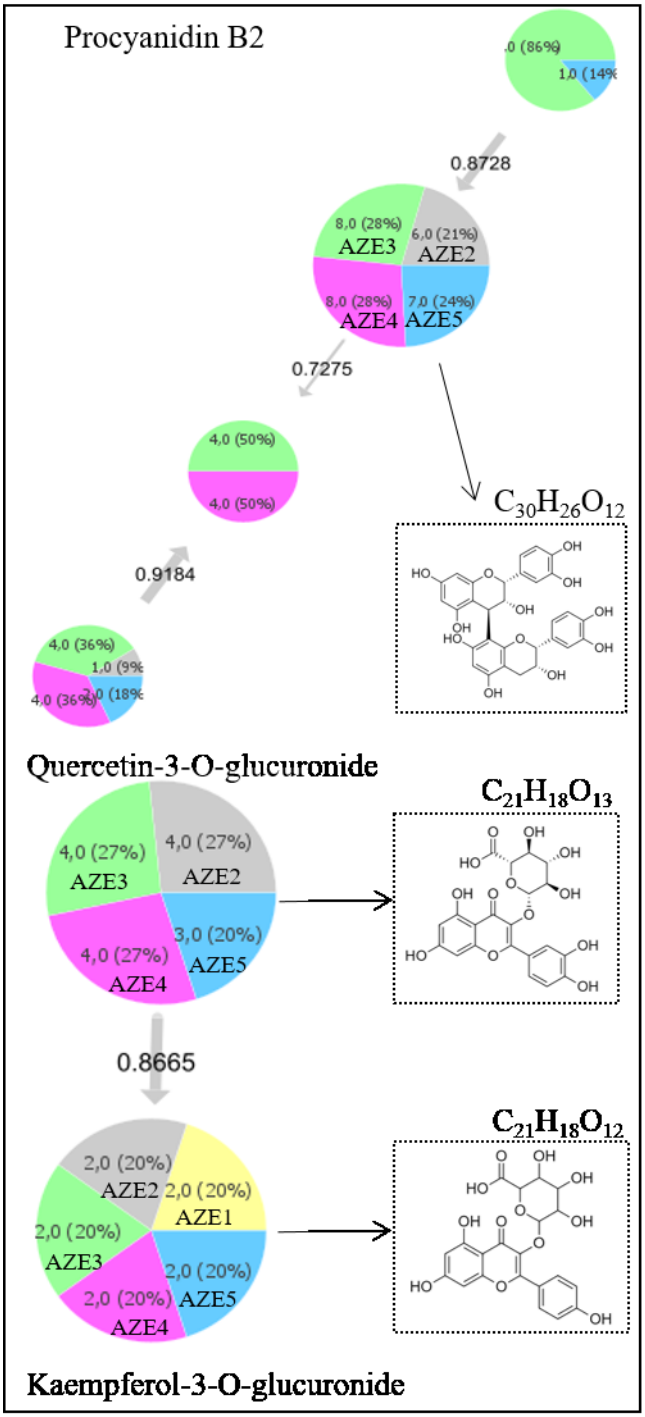

Fig. 5 Cytoscape view of Procyanidin B2, Quercetin-3-O-glucuronide and Kaempferol-3-O-glucuronide nodes annotated by GNPS. Cytoscape converted the abundance data obtained from each AZE TIC to percentages. AZE4 and AZE3 contribute with 28%, AZE5 with 24% and AZE2 with 21% of all Procyanidin B2 found in the molecular network. AZE2 AZE3 and AZE4 contribute with 27% and AZE5 with 20% of all Quercetin-3-O-glucuronide found in

the molecular network. All AZE contribute with 20% of all Kaempferol-3-O-glucuronide found in the molecular network

Quercetin aglycone is a well-known compound that exerts crucial benefits on cardiovascular health. GNPS annotated identified its derivative, quercetin-3-O-glucuronide (Fig. 5) as a putative compound for all extracts, except AZE1. Evidences show that this molecule is an effective inhibitor of reactive oxygen species (ROS)-associated inflammation and mitigating endothelial insulin resistance, stimulating the production of NO [27]. Furthermore, both quercetin aglycone and Q3OG are absorbed into plasma, but the derivative is less toxic and a more effective antioxidant [28].

Q3OG peak at 6.78 minutes presents fragment m/z 477 $[M-H]^-$ and one fragment at m/z 301 corresponding to the aglycone, after elimination of a glucuronide moiety $[M-H-176]^-$ as described in the literature [29]. The presence of other fragments derived from quercetin is in accordance with pathway described by Dueñas [30], and may be used to confirm Q3OG. Fragment at m/z 273 would correspond to the loss of the CO group $[M-28]^-$, m/z at 257 to the loss of CO_2, and m/z at 229 to the loss of both [30], characteristic of quercetin. Fragments m/z 151 and 179 are formed respectively by the A^- ring fragment released after RDA fission and the retro cyclization after fission [30]. These spectral data presented a 93% cosine score when compared to reference spectra of Q3OG.

Kaempferol metabolites, kaempferol-3-O-glucoside-3”-rhamnoside (K3OG3R – Fig. 6) and kaempferol-3-O-glucuronide (K3OG – Fig. 5) were annotated for all AZE at 6.77 and 6.87 minutes respectively. Indeed, the flavonols quercetin and kaempferol are present in plants as their metabolites in the sugar moieties forms, instead of aglycone form [31]. It is worth mentioning that kaempferol aglycone and K3OG (predominant form in human plasma) were pointed to be absorbed more efficiently than quercetin, even at small concentrations [32]. Additionally, Zaher [33] reported the inhibition of NF-κB as a rising mechanism in

minimizing cardiovascular diseases, and K3OG was one of the compounds involved in this process, as well as Q3OG.

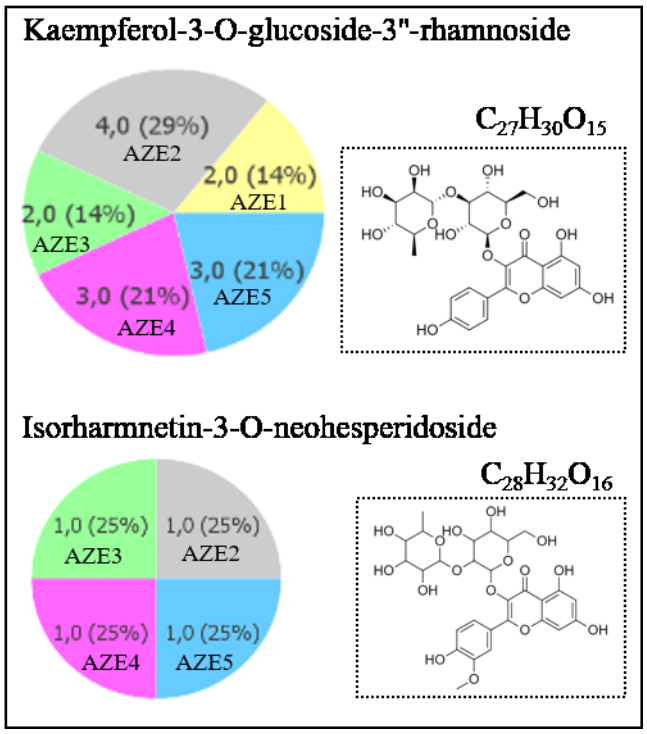

Fig. 6 Cytoscape view of Kaempferol-3-O-glucoside-3”-rhamnoside and Isorharmnetin-3-O-neohesperidoside nodes annotated by GNPS. Cytoscape converted the abundance data obtained from each AZE TIC to percentages. AZE2 contributes with 29%, AZE4 and AZE5 contribute with 21% and AZE1 and AZE3 with 14% of all Kaempferol-3-O-glucoside-3”-rhamnoside found in the molecular network. AZE2, AZE3, AZE4 and AZE5 contribute with 25% each one of all Isorharmnetin-3-O-neohesperidoside found in the molecular network

The fragmentation pattern of annotated K3OG3R is in accordance with the one described by Li [34], and presented a cosine score of 88% regarding reference spectra similarity. It is possible to find $[M–H]^-$ at m/z 593, $[M–H–162–146]^-$ at m/z 285 and $[M–H—162–146]^{-\bullet}$ at m/z 284 (losses of hexose and a deoxyhexose linked at the same position of the aglycone) [34]. The fragment at 447 m/z is a neutral loss of a deoxyhexose moiety from [M–

H]$^-$ at m/z 593, and the aglycone of kaempferol is confirmed by characteristic fragments at m/z 255 and 227 [34]. The K3OG had a score similarity of 81% with reference spectra at GNPS, and could be confirmed by comparison of obtained fragments with the ones described in the literature [35]: a base peak at 461 m/z in MS^1 and a base peak in 285 m/z in MS^2.

Isorhamnetin-3-O-6”-rhamnoside, also known as isorharmnetin-3-O-neohesperidoside (I3ON), derived from isorhamnetin (a metabolic product of quercetin) was also annotated. Isorhamnetin aglycone is known for its cardiovascular properties and I3ON (Fig. 6) presents antioxidant activity [36]. GNPS network annotated this compound at 6.90 minutes for all AZE, except AZE1, with a cosine score value of 84% when compared to reference spectra. Moreover, typical fragments could be identified to confirm this compound: deprotonated molecule $[M-H]^-$ at m/z 623 followed by the loss of $C_{12}H_{20}O_9$ producing the ion of aglycone at m/z 315, which m/z 151, a product after the Retro-Diels Alder (RDA) cleavage of m/z 315.

Surprisingly, pinocembrin (Fig. 7) was annotated for AZE4 and AZE5 at 10 minutes, but its content in AZE4 was more expressive in the MN than AZE5, which may explain the most potent vasodilator response of this extract. Pinocembrin, widely distributed in *Alpinia* species, has been reported as an inhibitor of angiotensin II-induced vasoconstriction [37], a modulator of inflammatory responses [38], and as a cardioprotective compound [39]. This compound presented 77% cosine score when compared with reference spectra, and could be confirmed due to the presence of typical fragments, as described by Simirgiortis [40]: m/z 255 $[M - H]^-$ and the product ion at m/z 213, due to a neutral loss of CO and CO_2 in C-ring, [M-H-CO-CO_2].

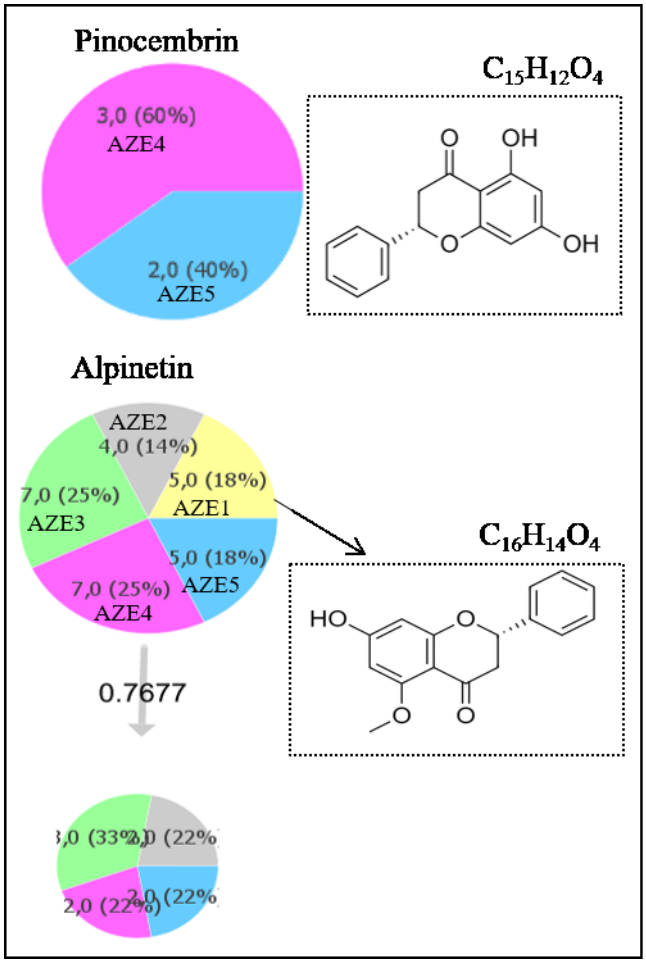

Fig. 7 Cytoscape view of Pinocembrin and Alpinetin nodes annotated by GNPS. Cytoscape converted the abundance data obtained from each AZE TIC to percentages. AZE4 contributes with 60% and AZE5 contributes with 40% of all Pinocembrin found in the molecular network. AZE3 and AZE4 contribute with 25%, AZE1 and AZE5 contribute with 18% and AZE2 with 14% of all Alpinetin found in the molecular network

Alpinetin (Fig. 7) is also frequently found in *Alpinia* gender, being annotated in all extracts at 8.84 and 10.90 minutes. These two possible retentions times is due to its isomeric structure, since it can be described as pinocembrin 5-methyl ether and co-occurs with the 7-methyl ether [41]. This compound may contribute to the anti-inflammatory potential of *Alpinia* leaves, a key factor for avoiding cardiovascular diseases [42]. A recent study [43] reported that pinocembrin and alpinetin (and its isomer) [41] induced vasodilation in isolated

coronary artery, through a mechanism in part dependent of endothelium involving NO production and an independent mechanism involving the blockage of Ca^{2+} channels. The cosine score for Alpinetin was 74% in comparison with reference spectra, and the fragmentation pathway found experimentally is in accordance with the one recently described [44]. It is possible to identify a base peak at m/z 269 $[M-H]^-$ in MS^1 and two radical anions at m/z 254 $[M–H–CH3]^-$, m/z 225 $[M–H – CO_2]^-$, and m/z 165 $[^{1,3}A–H]^–$ derived from Retro-Diels Alder rearrangement [44].

The underlying mechanisms of the vasodilator effect of the AZE remain to be elucidated, but a previous study demonstrated hydroethanolic extract from dried leaves of *Alpinia zerumbet* induces vasodilator effect in isolated MVB, an effect in part modulated by bradykinin B2 receptors and dependent on the activation of the NO-cyclic guanosine monophosphate (cGMP) pathway [11]. Almost all the annotated compounds as a putative composition for AZE4 follow this pathway, and these data may future help to elucidate and confirm the vasodilator mechanism of AZE.

Conclusion

In conclusion, this study has demonstrated that AZE4 was the most effective in producing vasodilation in the isolated MVB, with the highest polyphenol content. Molecular network, a trend in plant extracts data analysis, is an important and reliable tool for annotating compounds, confirmed by data comparison using classical search in literature. The main putative compounds annotated for all extracts are remarkable molecules with biological properties. Overall, this study leads us to the conclusion that the use of hydroethanolic extract obtained from fresh leaves of *Alpinia zerumbet* under heating may be useful for the treatment of cardiovascular diseases.

Experimental

Chemicals

Ethanol, acetic acid, acetonitrile, calcium carbonate ($CaCO_3$), sodium chloride (NaCl), potassium chloride (KCl), magnesium sulfate ($MgSO_4$), sodium bicarbonate ($NaHCO_3$), potassium phosphate monobasic (KH_2PO_4), calcium chloride ($CaCl_2$), ethylene diamine tetra acetic acid (EDTA), and glucose were purchased from Merck KGaA (Darmstadt, Germany). Norepinephrine, gallic acid, Folin-Ciocaulteau reagent, sodium formate, and acetylcholine were purchased from Sigma Chemical (St. Louis, MO, USA). Nitroglycerine was purchased from Innovatec Cristália (São Paulo, Brazil).

Experimental Biological Material

Leaves of *Alpinia zerumbet* were collected in Rio de Janeiro, RJ, Brazil. Plants were authenticated and a voucher specimen was deposited in the Herbarium Prof. Jorge Pedro Pereira Carauta of the Federal University of Rio de Janeiro State (UNIRIO), registered as HUNI5015.

Animals

Twelve-week-old male Wistar rats weighing 230 g – 250 g were obtained from the facilities of the Institute of Biology Roberto Alcântara Gomes (Rio de Janeiro, Brazil). The rats were fed with a standard rodent diet and allowed unrestricted access to water in a controlled environment, maintained at 18 ˚C –22 ˚C, 50 %–70 % relative humidity, and a 12-h light/dark cycle.

Methods

Leaves processing

Alpinia zerumbet leaves designed for fresh leaves extracts were properly cleaned and ground in a processor for the immediate extraction process. The other ones, designed for dried leaf extracts, underwent a natural drying process for ten days, through exposure to air at room temperature (20 - 22 ºC). After this period, leaves were ground and weighed until constant weight to confirm the effectiveness of the natural drying process. Finally, they were stored in a desiccator until use, at room temperature, protected from light.

Alpinia zerumbet extracts (AZE)

A total of 50g of AZ leaves was used to obtain each extract, with a total volume of 800mL. Filtration was performed using Whatman® #1 filter paper. A rotary evaporator at 65 °C (Fisatom Equipamentos Científicos Ltda, São Paulo, Brazil) under low pressure removed alcohol fraction of hydroethanolic extracts. Water content was removed by freeze-drying (LIOTOP model 202, São Paulo, Brazil) at - 30 ˚C to -40 ˚C under 200 mm Hg vacuum, and lyophilized samples were stored in a freezer until use.

The first extract (AZE1) was prepared with dried leaves in 50% hydroethanolic solution. This mixture was stored in an amber flask in a refrigerator for ten days, with 1-hour daily stirring on a mechanical stirrer, followed by filtration and lyophilization steps at the end of this cycle. Aqueous extract of dried leaves (AZE2) and fresh leaves (AZE3) were obtained after boil in distilled water for ten minutes, filtered, and stored in a freezer until the lyophilization process. Two 50% hydroethanolic extract using fresh leaves (AZE4) and dried leaves (AZE5) were prepared in 400 mL of boiling distilled water for ten minutes. After

cooling, 400 mL of ethanol was added to this infusion, and the extracts were stored following the same procedure applied to AZE1.

Isolation of mesenteric vascular bed and reactivity studies

To evaluate the vasodilator effect of the lyophilized extracts the mesenteric vascular bed of male Wistar rats (*n*=6/extract) was isolated following the method described by McGregor [45]. Summarily, rats were anesthetized with inhaled CO_2. The superior mesenteric artery was rapidly removed, cannulated, and continually perfused (4 mL/min) with physiological salt solution (PSS, nmol/L: 118 NaCl, 4.7 KCl, 2.5 $CaCl_2$, 1.2 $MgSO_4$, 1.2 KH_2PO_4, 25 $NaHCO_3$, 0.026 EDTA, and 6.0 glucose), oxygenated with 95% O_2-5% CO_2 at 37 °C, using a peristaltic pump (Model MINIPLUS 3, Gilson Inc., Middleton,WI, USA). A pressure transducer (Powerlab® 4/30, AD Instruments, Bella Vista, NSW 2153, Australia) recorded the changes in perfusion pressure (PP, mmHg) generated by arteriolar dilatation, continuously registered through LabChart7® (AD Instruments, Bella Vista, Australia) reader program.

All drugs were administrated as injections at the desired concentration, directly into the perfusion stream, close to the vascular cannula. After a 30-minute equilibration period, MVB was preconstricted with KCl (120 μmol), regularly every ten minutes, until consistent responses were obtained. Subsequently, basal perfusion pressure was elevated (80–100 mmHg) by adding norepinephrine (NE; 30 μM) to the perfusion solution. After the vasopressor response of NE reached a constant plateau, acetylcholine (ACh, 10 pmol) and nitroglycerine (NG, 10 nmol) were infused to test the viability of endothelium and smooth muscle cells, respectively. Increasing doses of the AZE (0.1-300 μg), properly dissolved in MilliQ® water (Merck KGaA, Darmstadt, Germany) were injected at the perfusion system to evaluate its vasodilator effect. The vasodilator effect was expressed as a percentage decrease of the pressor effect of NE.

Determination of total polyphenols by the Folin-Ciocaulteau method

Total polyphenols content (TPC) in AZE was assessed using the colorimetric method described by Singleton & Rossi [46]. A calibration curve of gallic acid (GA) solutions was prepared using concentrations of 0.08, 0.13, 0.25, 0.50, 0.76 and 1.00 mg/mL. Aliquots of 200 µL of calibration solutions, blank and properly diluted AZE (2mg/mL) were tested. The absorbance was measured in UV/VIS spectrophotometer at 765 nm (GE Ultrospec 2100 Pro®, GE Healthcare UK Limited, Buckinghamshire, UK) and the TPC in AZE (analyzed in triplicates) was determined from the linear regression equation of calibration curve: Absorbance = 0.004464*Concentration + 0.2518, R^2=0.999. Results were expressed as mg of GA equivalent (GAE)/g of AZE.

UHPLC/ESI-QTOF-MS analysis

Each AZE was weighed accurately and dissolved in 50% methanolic solution (5mg/mL), followed by 10 min sonication and centrifuged. After those steps, samples were diluted in water to prepare a 1mg/mL stock solution.

Qualitative analysis by UHPLC/ESI-QTOF-MS was performed with a Shimadzu Nexera X2® ultra-fast liquid chromatography (UHPLC) (Shimadzu Corp., Kyoto, Japan). The separation was carried out on an ODS Hypersil C18 column (2,1 mm x 150mm, 3 µm, Thermo Fisher Scientific, Waltham, MA USA) and a Phenomenex® (Torrence, CA, USA) precolumn C18 (4mm x 3,0 mm) at 40˚C. The mobile phase consisted of 0.1% acetic acid (v/v) in water (A) and acetonitrile (B) using a linear gradient from 0 to 10% B (0–13 min), 10 to 100% B (13–16 min), 100% B (16–17 min), 100 to 10% B (17–25 min), stop time at 25 minutes. The injected volume was 5 µL, with the flow rate kept at 0.2 mL/min.

Detections were performed by a maXis Impact II® quadrupole time-of-flight (Q-TOF) mass spectrometry (MS) (Bruker Daltonik GmbH, Bremen, Germany) equipped with an electrospray ionization (ESI) source. The Q-TOF-MS operated in full scan mode, and the mass range was set to m/z 100–800 in negative ion mode. The acquisition type was Auto MS/MS (data-dependent) mode, at a rate of five spectra/sec. The conditions of the mass spectrometry were as follows. Spectra rate: 1 Hz; Dry temperature: 200ºC; Capillary voltage: 5000 V; Collision energy: 10 - 60V; End plate offset: -500 V; Quadrupole low mass: 80 m/z; Nebulizer pressure: 2.0 bar; Dry gas: 8.0 L/min. External calibration with a 0.1 mmol sodium formate/acetonitrile 1:1 solution was performed at the beginning of each analysis.

Data processing

All raw data files obtained from AZE analysis were converted to .mzXML by MSConvert, Proteo Wizard Software (version 3.0) [47] (http://proteowizard.sourceforge.net), to be preprocessed with MZMine (version 2.53) [48] with the following parameters. Mass detection: MS level 1; Mass Detector, centroid; Noise level, 1000; Retention time, Auto Range. MS level 2; Mass Detector, centroid; Noise level, 10. Retention time, Auto Range. ADAP Chromatogram builder (49): MS level 1; Retention time, Auto Range; Min group size, 5; Group intensity threshold, 3000; Min highest intensity, 150; m/z tolerance 0.01 or 10 ppm. Chromatogram deconvolution: Baseline cut-off; min peak height, 3000; Peak duration range (min), 0.005-2; Baseline level, 1000; m/z center calculation: median; m/z range for MS^2 scan pairing (Da), 0.02; RT range for MS^2 scan pairing (min), 0.015. Isotopic peak grouper: m/z tolerance 0.02 m/z or 10 ppm; Retention time tolerance 0.1 min absolute (min); Maximum charge, 2; Representative isotope, most intense. Join aligner: m/z tolerance, 0.01 m/z or 10 ppm; Weight for m/z 75; Retention time tolerance, 0.1 absolute (min); Weight for RT 25. Feature list rows filter: Minimum peaks in a row, 2; Minimum peaks in an isotope pattern, 2;

Keep only peaks with MS2 scans (GNPS). Gap filling, peak finder: Intensity, 10%; m/z tolerance, 0.01 m/z or 10 ppm; Retention time tolerance, 0.2 absolute (min). A feature table with all extracted mass spectral data was exported to .csv format, aggregated MS2 fragmentation data and converted to .mgf format.

These files were uploaded into METABOLOMICS-SNETS-V2 workflow from Global Natural Product Social Molecular Networking (GNPS) and analyzed with GNPS platform (http://gnps.ucsd.edu) [50]. The data were filtered by removing all MS/MS fragment ions within +/- 17 Da of the precursor m/z. MS/MS spectra were window filtered by choosing only the top six fragment ions in the +/- 50Da window throughout the spectrum. The precursor ion mass tolerance was set to 0.02 Da and an MS/MS fragment ion tolerance of 0.02 Da. A molecular network (MN) was then created, where edges were filtered to have a cosine score above 0.7 and more than six matched fragments. Further, edges between two nodes were kept in the network if and only if each of the nodes appeared in each other's respective top ten most similar nodes. Finally, the maximum size of a molecular family was set to 100, and the lowest-scoring edges were removed from molecular families until the molecular family size was below this threshold. The spectra in the network were then searched against GNPS' spectral libraries. The library spectra were filtered in the same manner as the input data: all matches kept between network spectra and library spectra were required to have a score above 0.7 and at least six matched peaks (50). A job for all five AZE samples was carried out at Metabolomics-SVNETS-V2 workflow on GNPS platform, each extract allocated into different groups (G1 – G5), including blank analysis (methanol) on G6. Library annotations were obtained from the comparison between MS^2 spectra with GNPS and MassBank spectral libraries. The resulting MN is available at: https://gnps.ucsd.edu/ProteoSAFe/status.jsp?task=59981840eb014f44903aee3008f48d00.

The final step on data analysis, the molecular network visualization, was achieved by uploading the spectral network to Cytoscape 3.8.2 [51] to improve MN visualization. Nodes were labeled with annotated compound names, represented by a pie chart, where the percentage of contribution from each extract could be compared, identified by different colors. The edges were labelled with cosine scores between connected nodes, and the edge thickness is proportional to cosine score.

Statistical analysis

Data are shown as the mean and standard error of the mean. Differences among groups were analyzed by one-way analysis of variance (one-way ANOVA) and post-hoc test of Tukey using GraphPad Prism version 6.0 (GraphPad Software, San Diego, USA). Besides, differences between two groups were evaluated by the unpaired Student's t-Test using GraphPad Prism version 6.0 (GraphPad Software, San Diego, USA). P values less than or equal to 0.05 were accepted as statistically significant.

Acknowledgements

The authors are grateful to the National Council of Scientific and Technological Development (CNPq, nº 444983/2014-7), Rio de Janeiro State Research Agency (FAPERJ, nº E-26/202.913/2017), and Coordination for the Improvement of Higher Education Personnel (CAPES).

Compliance with ethical standards

Ethical statement

This study was carried out in compliance with the guidelines of the Ethics Committee for the Care and Use of Experimental Animals of the Institute of Biology Roberto Alcântara Gomes, Rio de Janeiro, Brazil (protocol No. 52/2016).

Conflict of interest

The authors declare that they have no conflict of interest.

References

1. Saúde M da, ANVISA. Monografia das espécies Alpinia speciosa E Alpinia zerumbet (Galanga). Vol. 5. Brasília; 2014.
2. World Health Organization. A global brief on hypertension: silent killer, global public health crisis: World Health Day 2013. 2013. https://apps.who.int/iris/handle/10665/79059. Accessed April 27 2021.
3. Nishidono Y, Okada R, Iwama Y, Okuyama T, Nishizawa M, Tanaka K. Anti-inflammatory kavalactones from Alpinia zerumbet. Fitoterapia. 2020;140:104444. doi: 10.1016/j.fitote.2019.104444.
4. Chen Y, Li D, Xu Y, Zhang Y, Tao L, Li S, et al. Essential oils from Fructus A. zerumbet protect human aortic endothelial cells from apoptosis induced by Ox-LDL in vitro. Evidence-based Complement Altern Med. 2014;2014. doi: 10.1155/2014/956824.
5. Chompoo J, Upadhyay A, Kishimoto W, Makise T, Tawata S. Advanced glycation end

products inhibitors from Alpinia zerumbet rhizomes. Food Chem. 2011;129(3):709–15. doi: 10.1016/j.foodchem.2011.04.034.

6. Chompoo J, Upadhyay A, Fukuta M, Tawata S. Effect of Alpinia zerumbet components on antioxidant and skin diseases-related enzymes. BMC Complement Altern Med. 2012;12.

7. Chompoo J, Upadhyay A, Gima S, Fukuta M, Tawata S. Antiatherogenic properties of acetone extract of Alpinia zerumbet seeds. Molecules. 2012;17(6):6237–48. doi: 10.3390/molecules17066237.

8. Cunha GH Da, Moraes MO De, Fechine FV, Frota Bezerra FA, Silveira ER, Canuto KM, et al. Vasorelaxant and antihypertensive effects of methanolic fraction of the essential oil of Alpinia zerumbet. Vascul Pharmacol. 2013;58(5–6):337–45. doi: 10.1016/j.vph.2013.04.001.

9. Tao L, Shuai H, Chun X. Phytomedicine Endothelium-dependent vasodilatation effects of the essential oil from Fructus Alpiniae Zerumbet (EOFAZ) on rat thoracic aortic rings in vitro. Eur J Integr Med. 2013;20(5):387–93. doi: 10.1016/j.phymed.2012.12.014.

10. Panche AN, Diwan AD, Chandra SR. Flavonoids: An overview. J Nutr Sci. 2016;5:1–15. doi: 10.1017/jns.2016.41.

11. de Moura RS1, Emiliano AF, de Carvalho LC, Souza MA, Guedes DC, Tano T RA. Antihypertensive and endothelium-dependent vasodilator effects of Alpinia zerumbet, a medicinal plant. J Cardiovasc Pharmacol. 2005;46(3):288–94.

12. Stoclet JC, Chataigneau T, Ndiaye M, Oak MH, El Bedoui J, Chataigneau M, et al. Vascular protection by dietary polyphenols. Eur J Pharmacol. 2004;500:299–313. doi: 10.1016/j.ejphar.2004.07.034.

13. Curin Y, Andriantsitohaina R. Polyphenols as potential therapeutical agents against

cardiovascular diseases. Pharmacol Reports. 2005;57:97–107.

14. Kashi DS, Shabir A, Da Boit M, Bailey SJ, Higgins MF. The efficacy of administering fruit-derived polyphenols to improve health biomarkers, exercise performance and related physiological responses. Nutrients. 2019;11(10):1–13. doi: 10.3390/nu11102389.

15. Verardo G, Duse I, Callea A. Analysis of underivatized oligosaccharides by liquid chromatography/electrospray ionization tandem mass spectrometry with post-column addition of formic acid. Rapid Commun Mass Spectrom. 2009;23:1607–1618. doi: 10.1002/rcm.4047.

16. Calvano CD, Cataldi TRI, Kögel JF, Monopoli A, Palmisano F, Sundermeyer J. Structural characterization of neutral saccharides by negative ion MALDI mass spectrometry using a superbasic proton sponge as deprotonating matrix. J Am Soc Mass Spectrom. 2017;28(8):1666–75. doi: 10.1007/s13361-017-1679-y.

17. Tsao R. Chemistry and biochemistry of dietary polyphenols. Nutrients. 2010;2(12):1231–46. doi: 10.3390/nu2121231.

18. Escobar-Avello D, Lozano-Castellón J, Mardones C, Pérez AJ, Saéz V, Riquelme S, et al. Phenolic profile of grape canes: Novel compounds identified by LC-ESI-LTQ-orbitrap-MS. Molecules. 2019;24(20):1–21. doi: 10.3390/molecules24203763.

19. Carnevale R, Nocella C, Schiavon S, Cammisotto V, Cotugno M, Forte M, et al. Synergistic beneficial effects of natural activators of autophagy on endothelial cells and platelets. British Journal of Pharmacology. 2021. doi: 10.1111/bph.15399.

20. Mangels DR, Mohler ER. Catechins as potential mediators of cardiovascular health. Arterioscler Thromb Vasc Biol. 2017;37(5):757–63. doi: 10.1161/ATVBAHA.117.309048.

21. Chen XQ, Hu T, Han Y, Huang W, Yuan HB, Zhang YT, et al. Preventive effects of

catechins on cardiovascular disease. Molecules. 2016;21(12):1–7. doi: 10.3390/molecules21121759.

22. Coșarcă S, Tanase C, Muntean DL. Therapeutic aspects of catechin and its derivatives – an update. Acta Biol Marisiensis. 2019;2(1):21–9. doi: 10.2478/abmj-2019-0003.

23. Novakovic A, Marinko M, Jankovic G, Stojanovic I, Milojevic P, Nenezic D, et al. Endothelium-dependent vasorelaxant effect of procyanidin B2 on human internal mammary artery. Eur J Pharmacol. 2017;807:75–81. doi: 10.1016/j.ejphar.2017.04.015.

24. Kopustinskiene DM, Savickas A, Vetchý D, Masteikova R, Kasauskas A, Bernatoniene J. Direct effects of (-)-epicatechin and procyanidin B2 on the respiration of rat heart mitochondria. Biomed Res Int. 2015;2015. doi: 10.1155/2015/232836.

25. Jankovic G, Marinko M, Milojevic P, Stojanovic I, Nenezic D, Kanjuh V, et al. Mechanisms of endothelium-dependent vasorelaxation induced by procyanidin B2 in venous bypass graft. J Pharmacol Sci. 2020;142(3):101–8. doi: 10.1016/j.jphs.2019.11.006.

26. Maldini M, Montoro P, Piacente S, Pizza C. ESI-MS, ESI-MS/MS Fingerprint and LC-ESI-MS Analysis of Proathocyanidins from Bursera simaruba Sarg Bark. 2009;4(12):1671–4.

27. Guo XD, Zhang DY, Gao XJ, Parry J, Liu K, Liu BL, et al. Quercetin and quercetin-3-O-glucuronide are equally effective in ameliorating endothelial insulin resistance through inhibition of reactive oxygen species-associated inflammation. Mol Nutr Food Res. 2013;57(6):1037–45. doi: 10.1002/mnfr.201200569.

28. Yin H, Ma J, Han J, Li M, Shang J. Pharmacokinetic comparison of quercetin, isoquercitrin, and quercetin-3-O-β-Dglucuronide in rats by HPLC-MS. PeerJ. 2019;2019(3):1–17. doi: 10.7717/peerj.6665.

29. KajdŽanoska M, Gjamovski V, Stefova M. HPLC-DAD-ESI-MSn identification of phenolic compounds in cultivated strawberries from Macedonia. Maced J Chem Chem Eng. 2010;29(2):181–94.

30. Dueñas M, Mingo-Chornet H, Pérez-Alonso JJ, Di Paola-Naranjo R, González-Paramás AM, Santos-Buelga C. Preparation of quercetin glucuronides and characterization by HPLC-DAD-ESI/MS. Eur Food Res Technol. 2008;227(4):1069–76. doi: 10.1007/s00217-008-0821-2.

31. Dabeek WM, Marra MV. Dietary quercetin and kaempferol: Bioavailability and potential cardiovascular-related bioactivity in humans. Nutrients. 2019;11(10). doi:10.3390/nu11102288.

32. DuPont MS, Day AJ, Bennett RN, Mellon FA, Kroon PA. Absorption of kaempferol from endive, a source of kaempferol-3-glucuronide, in humans. Eur J Clin Nutr. 2004;58(6):947–54. doi:10.1038/sj.ejcn.1601916.

33. Polygonoides C, Targeting LF, Zaher AM, Ahmed MAM, Mohamed NM. Anti-inflammatory activity of the food plant Calligonum polygonoides L. flavonoids targeting NF-κB. Bull Pharm Sci Assiut. 2020;43(2):157–64.

34. Li ZH, Guo H, Xu W Bin, Ge J, Li X, Alimu M, et al. Rapid Identification of flavonoid constituents directly from PTP1B inhibitive extract of raspberry (Rubus idaeus L.) leaves by HPLC-ESI-QTOF-MS-MS. J Chromatogr Sci. 2016;54(5):805–10.

35. Kumar S, Singh A, Kumar B. Identification and characterization of phenolics and terpenoids from ethanolic extracts of Phyllanthus species by HPLC-ESI-QTOF-MS/MS. J Pharm Anal [Internet]. 2017;7(4):214–22. doi: 10.1016/j.jpha.2017.01.005.

36. Rashid MI, Fareed I, Laboratories H, Aziz H, Ehsan N. Plant and Human Health, Volume 2. Plant Hum Heal Vol 2. 2019.

37. Li L, Pang X Bin, Chen BN, Gao L, Wang L, Wang SB, et al. Pinocembrin inhibits

angiotensin II-induced vasoconstriction via suppression of the increase of [Ca2+] and ERK1/2 activation through blocking AT1R in the rat aorta. Biochem Biophys Res Commun. 2013;435(1):69–75. doi: /10.1016/j.bbrc.2013.04.039.

38. Soromou LW, Chu X, Jiang L, Wei M, Huo M, Chen N, et al. In vitro and in vivo protection provided by pinocembrin against lipopolysaccharide-induced inflammatory responses. Int Immunopharmacol. 2012;14(1):66–74. doi: 10.1016/j.intimp.2012.06.009.

39. Zheng Y, Wan G, Yang B, Gu X, Lin J. Cardioprotective natural compound pinocembrin attenuates acute ischemic myocardial injury via enhancing glycolysis. Oxid Med Cell Longev. 2020;2020. doi: 10.1155/2020/4850328.

40. Simirgiotis MJ, Benites J, Areche C, Sepu B. Antioxidant capacities and analysis of phenolic compounds in three endemic nolana species by HPLC-PDA-ESI-MS. Molecules. 2015;20(6):11490–507. doi: 10.3390/molecules200611490.

41. Harborne, Jeffrey B., Marby, Helga, Marby TJ. The Flavonoids. 1st ed. Springer US; 1982. 1204 p.

42. Ma XN, Xie CL, Miao Z, Yang Q, Yang XW. An overview of chemical constituents from Alpinia species in the last six decades. RSC Adv. 2017;7(23):14114–44. doi: 10.1039/c6ra27830b.

43. Adhikari D, Gong DS, Oh SH, Sung EH, Lee SO, Kim DW, et al. Vasorelaxant effect of Boesenbergia rotunda and its active ingredients on an isolated coronary artery. Plants. 2020;9(12):1–13. doi: 10.3390/plants9121688.

44. Zhao X, Zhang S, Liu D, Yang M, Wei J. Analysis of flavonoids in Dalbergia odorifera by Ultra-Performance Liquid Chromatography with tandem mass spectrometry. Molecules. 2020;25(2). doi: 10.3390/molecules25020389.

45. Mcgregor BYDD. The effect of sympathetic nerve stimulation on vasoconstrictor

responses in perfused mesenteric blood vessels of the rat. J Physiol. 1965;177:21–30.

46. Singleton VL, Rossi JAJ. Colorimetry of total phenolics with phosphomolybdic-phosphotungstic acid reagents. Am J Enol Vitic. 1965;16:144–58.

47. Kessner D, Chambers M, Burke R, Agus D, Mallick P. ProteoWizard: Open source software for rapid proteomics tools development. Bioinformatics. 2008;24(21):2534–6. doi: 10.1093/bioinformatics/btn323.

48. Pluskal T, Castillo S, Villar-Briones A, Orešič M. MZmine 2: Modular framework for processing, visualizing, and analyzing mass spectrometry-based molecular profile data. BMC Bioinformatics. 2010;11.

49. Myers OD, Sumner SJ, Li S, Barnes S, Du X. One Step Forward for Reducing False Positive and False Negative Compound Identifications from Mass Spectrometry Metabolomics Data: New Algorithms for Constructing Extracted Ion Chromatograms and Detecting Chromatographic Peaks. Anal Chem. 2017;89(17):8696–703. doi:

50. Wang M, Carver JJ, Phelan V V., Sanchez LM, Garg N, Peng Y, et al. Sharing and community curation of mass spectrometry data with Global Natural Products Social Molecular Networking. Nat Biotechnol. 2016;34(8):828–37. doi: 10.1021/acs.analchem.7b00947.

51. Shannon P, Markiel A, Ozier O, Baliga NS, Wang JT, Ramage D, et al. Cytoscape: A software environment for integrated models. Genome Res. 2003;13(22):2498–504. doi: http://ci.nii.ac.jp/naid/110001910481/